

Full Paper

Ultrasound Assisted Green Synthesis of 3-(4-(dimethylamino) phenyl)-1-phenylprop-2-en-1-one and its Heterocyclics Derived from Hydrazine, Urea and Thiourea as Corrosion Inhibitor for Mild Steel in 1M HCl

Chandra Bhan Verma¹, Mareddy Jayanth Reddy², Mumtaz Ahmad Quraishi^{1*}

¹*Department of Chemistry, Indian Institute of Technology, Banaras Hindu University, Varanasi 221005, India*

²*Department of Metallurgical Engineering, Indian Institute of Technology, Banaras Hindu University, Varanasi 221005, India*

* Corresponding Author, Tel.: +91-9307025126; Fax: +91- 542- 2368428

E-Mail: maquraishi.apc@itbhu.ac.in, maquraishi@rediffmail.com

Received: 1 July 2014 / Accepted: 9 October 2014 / Published online: 31 October 2014

Abstract- The purpose of present study was to investigate the corrosion inhibition property of 3-(4-(dimethylamino) phenyl)-1-phenylprop-2-en-1-one(a chalcone, INH-1) derived from condensation of acetophenone and 4, 4- dimethylamino benzaldehyde and three heterocyclics derived from this using Hydrazine (INH-2), Urea (INH-3) and Thiourea (INH-4) on mild steel (MS) in 1M HCl by weight loss and electrochemical methods. It was found that inhibition efficiency increases with inhibitor concentration and maximum efficiency was obtained at 25 ppm. Among the studied inhibitors, INH-4 shows the best inhibition efficiency of 98.26 %. Variation of impedance parameters (Rct and Cdl) suggests the formation of protective film of inhibitors on MS surface. The adsorption of inhibitors on MS surface was also studied using Scanning Electron Microscopy (SEM) and Energy Dispersive X-ray spectroscopy (EDX) techniques. The potentiodynamic study reveals that all studied compounds are of mixed type. The adsorption of inhibitors on MS surface was found to follow the Langmuir adsorption isotherm. The weight loss experiment was also performed at different temperature to study the effect of temperature on corrosion rate (CR) and evaluated some thermodynamic parameters.

Keywords- Chalcone, Mild Steel EIS, Corrosion, 1M HCl, SEM-EDX

1. INTRODUCTION

Mild Steel (MS) is a promising material used for various industrial applications such as reactors, petrochemical process devices, boilers, drums, and heat exchangers. However, exposal of MS with aqueous acidic solution during descaling, acid pickling, and acid treatment in oil industries causes corrosion. In efforts to diminish electrochemical corrosion, the primary strategy is to isolate the metal from corrosive media. There are several methods are available but the use of chemical corrosion inhibitors is the most appropriate and economical way to achieve this target [1]. Most of the known corrosion inhibitors are heterocyclic organic compounds containing mostly Nitrogen, Oxygen and Sulfur [2-9]. The existing data show that most organic inhibitors act by adsorption on the metal surface in which polar groups acting as adsorption centers [10]. Besides their applications in synthesis of various heterocyclic compounds having therapeutic [11-12] properties, chalcones possess potential application in science of art and electronics such as printing circuit and color filters. Recently, the inhibition properties of chalcones synthesized in presence of appropriate condensation reagents were studied in aggressive acidic media [13-14].

In the view of the various biological and pharmacological applications, in the present study we have synthesized a chalcone from condensation of acetophenone with 4, 4-dimethyl amino benzaldehyde namely (E)-3-(4-(dimethylamino) phenyl)-1-phenylprop-2-en-1-one, (INH-1) from which three heterocyclic compounds namely N, N-dimethyl-4-(3-phenyl-4, 5-dihydroisoxazol-5-yl)aniline (INH-2), 6-(4-(dimethylamino) phenyl)-4-phenyl-5, 6-dihydro-4H-1, 3-oxazin-2-amine (INH-3), and 6-(4-(dimethylamino) phenyl)-4-phenyl-5, 6-dihydro-4H-1, 3-thiazin-2-amine (INH-4) were derived using hydrazine, urea, and thiourea, respectively. The corrosion inhibition property of synthesized chalcone and heterocyclic compounds were investigated using weight loss, electrochemical and SEM/EDX methods. The SEM and EDX spectra of MS surface were recorded in order to study the changes in surface morphology in absence and presence inhibitors.

2. EXPERIMENTAL

2.1. Preparation of Solutions and Samples

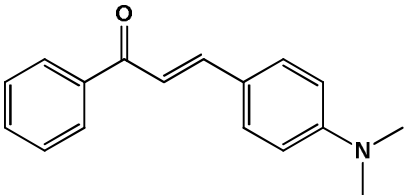
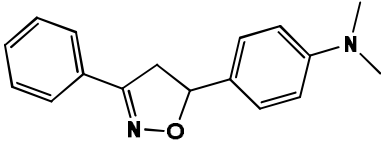
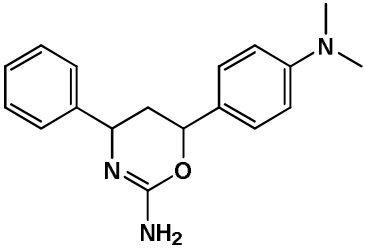
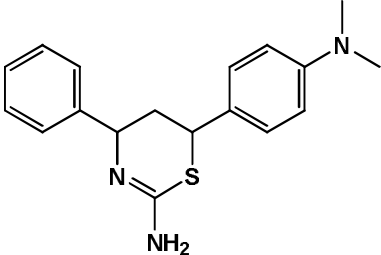
The corrosion tests were performed on MS specimens having composition (wt.%): C=0.076, Mn=0.192, P=0.012, Si=0.026, Cr=0.050, Al=0.023, Cu=0.123 and remainder Fe. Prior to weight loss and electrochemical experimenters, the MS specimens were abraded with SiC abrasive papers of grades 600, 800, 1000, and 1200, respectively, washed with acetone, cleaned in absolute ethanol, dried at ambient temperature, and stored in moisture-free desiccators before use in corrosion studies. MS specimens of size $2.5 \times 2 \times 0.025$ and $8 \times 1 \times 0.025$ cm³ were used for weight loss and electrochemical measurements, respectively.

Analytical-reagent- (AR-, 37%) grade HCl was diluted with doubly distilled water to prepare test solution (1M HCl).

2.2. Inhibitors Synthesis

The chalcone and its heterocyclics derivatives were synthesized as describe earlier in literature [15]. The synthesis was also achieved by modified method using ultrasonication technique according to scheme given in Fig. 1. In the modified method same reaction mixture used in previous synthesis was irradiated in ultrasonic bath for 25-30 minutes at 40°C.

Table 1. Molecular structure and analytical data of studied inhibitors

Inhibitor	Structure	Analytical data
(E)-3-(4-(dimethylamino) phenyl)-1-phenylprop-2-en-1-one (INH-1) (PPZ-1)		mp: 96; FT-IR (AT-IT, cm ⁻¹): ν 745, 778, 751.6, 850.6, 987.9, 1029.1, 1065, 1125.5, 1370, 1432.4, 1511.8, 1595, 1610.8, 1647.2, 2678.4, 2971.1
N, N-dimethyl-4-(3-phenyl-4, 5-dihydroisoxazol-5-yl) aniline (INH-2) (PPZ-2)		mp; 76
6-(4-(dimethylamino) phenyl)-4-phenyl-5, 6-dihydro-4H-1, 3-oxazin-2-amine (INH-3)		mp: 65; FT-IR (AT-IR, cm ⁻¹): ν 7119, 760, 814.4, 1019.5, 1124.3, 1216.8, 1611.2, 2677.9, 3394.2
6-(4-(dimethylamino) phenyl)-4-phenyl-5, 6-dihydro-4H-1, 3-thiazin-2-amine (INH-4)		mp: 73; FT-IR (AT-IR, cm ⁻¹): ν 685, 710.2, 763.2, 801.1, 1002.3, 1169, 1226.6, 1370.8, 1613.9, 1657, 2878.3, 3226., 3409.2

Progress of the reaction was marked by change in color and column chromatographic technique. Completion of reaction and purity of the products was confirmed by thin-layer

chromatography with a mixture of ethyl acetate/n-hexane (20:80) using the SiliaPlate TLC Plates–Aluminum (Al) Silica. The melting points of compounds were determined in open capillaries and matched with literature values [15]. The systematic name, chemical structure, abbreviation used for chalcone and heterocyclics, melting point and FT-IR spectral of is given in Table 1.

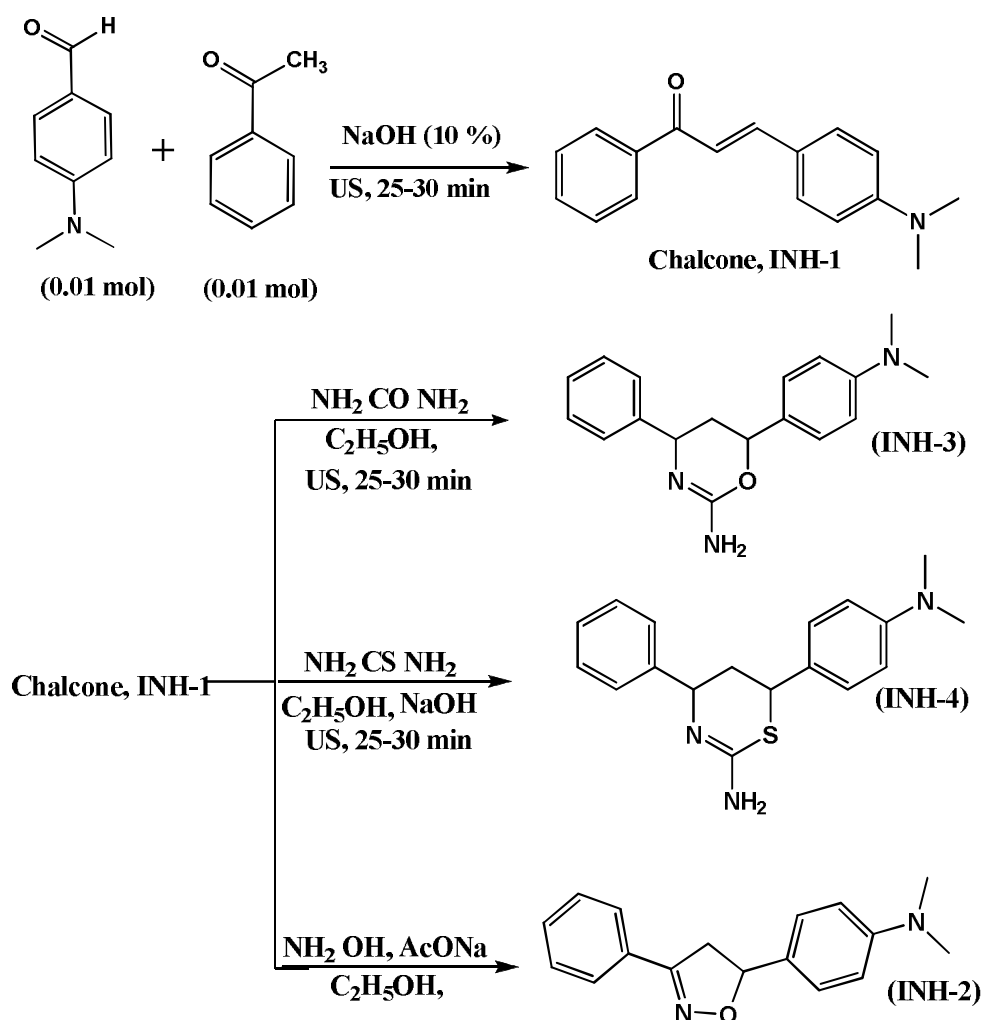


Fig.1. Synthetic scheme of inhibitors

2.3. Weight Loss Measurements

The Weight loss experiments were performed on MS specimens with exposed area $2.5 \times 2 \times 0.025 \text{ cm}^3$ for 3h immersion time at 308 K. All experiments were triply performed and

mean values were reported. Corrosion rate C_R ($\text{mg cm}^{-2} \text{h}^{-1}$) was calculated using following relation:

$$C_R = \frac{W}{At} \quad (1)$$

where W is the average weight loss of three parallel MS strips, A the exposed area of mild strip and t is immersion time (3h). From this calculated corrosion rate (C_R), the inhibition efficiency (η %) and surface coverage (θ) were calculated using following relationship:

$$\eta \% = \frac{C_R - C_{R(i)}}{C_R} \times 100 \quad (2)$$

$$\theta = \frac{C_R - C_{R(i)}}{C_R} \quad (3)$$

Where C_R and $C_{R(i)}$ are the corrosion rate values in absence and presence of inhibitors respectively.

2.4. Electrochemical Measurements

A conventional three-electrode cell was used to carry out all electrochemical measurements. The working electrode was a MS specimen with a geometric area of 1 cm^2 . The auxiliary electrode having exposed area 1 cm^2 was a high purity platinum foil and the reference electrode was a saturated calomel electrode (SCE). Prior to each electrochemical measurements the working electrode was polished with 1200 emery paper, cleaned ultrasonically, degreased with acetone, rinsed with deionized water and air-dried. All electrochemical measurements were carried out using a Gamry Potentiostat/Galvanostat (Model G-300) which consists of EIS software Gamry Instruments Inc., USA. Echem Analyst 5.0 software package was used to fit the electrochemical data. All the experiments were performed on MS specimens after for 30 min immersion time in 1M HCl in absence and presence of optimum concentrations of inhibitors.

The potentiodynamic behavior of MS in absence and presence of optimum concentration of inhibitors were studied by recording the cathodic and anodic polarization curves in the potential range of -0.250 and $+0.250 \text{ V}$ at open circuit potential (OCP) with a scan rate of 1 mV s^{-1} . From extrapolation of linear segments of polarization curves corrosion current densities (I_{corr}) were calculated and corrosion inhibition efficiency was calculated using following relationship:

$$\eta \% = \left(1 - \frac{I_{\text{corr}(i)}}{I_{\text{corr}}} \right) \times 100 \quad (4)$$

where $I_{\text{corr}(i)}$ and I_{corr} are corrosion current density without and with presence of inhibitors, respectively.

Electrochemical impedance spectroscopy (EIS) was carried out at the open-circuit potential in the frequency range 100 kHz to 0.01 Hz with a sine wave of 10 mV amplitude. Charge transfer resistance (R_{ct}) was calculated from the diameters of semicircle in Nyquist plots. From Charge transfer resistance inhibition efficiency was calculated using following equation:

$$\eta \% = \frac{R_{\text{ct}(i)} - R_{\text{ct}(0)}}{R_{\text{ct}(i)}} \times 100 \quad (5)$$

where $R_{\text{ct}(0)}$ and $R_{\text{ct}(i)}$ are the charge-transfer resistance values in absence and presence of inhibitors, respectively.

2.5. Surface Characterization

The MS specimens were immersed in 1M HCl for three hour and after elapsed time the specimens were taken out, washed with distilled water, degreased with acetone, ultrasonically cleaned with absolute ethanol, dried at ambient temperature, and mechanically cut into 1 cm² sizes for SEM and EDX investigations. Surface morphology studies were carried out at 500× magnification on a *Ziess Evo 50 XVP* instrument. Chemical composition of the corrosion products was recorded by an EDX detector coupled to the SEM.

3. RESULTS AND DISCUSSION

3.1. Weight Loss Measurements

3.1.1. Effect of Inhibitor Concentration

In order to evaluate the effect of inhibitor concentration on inhibition efficiency, weight loss experiments were performed on MS specimens for 3h immersion time at 308K. The weight loss parameters such as corrosion rate (C_R), inhibition efficiency ($\eta\%$) and corresponding surface coverage (θ) are given in Table 2. It is apparent from the Table 2 that inhibition efficiency increases with inhibitor concentration. The increase in inhibition performance with concentration can be attributed to an increase in the number of inhibitor molecules adsorbed on the metal surface, which separate the MS from the acid solution, resulting in the retardation of metal dissolution [16]. From Table 2, it is clear that the order of

inhibition efficiency of studied inhibitors is as follows: INH-4 > INH-3 > INH-2 > INH-1. The variation of inhibition efficiency with concentration is shown in Fig. 2(a).

Table 2. Parameters obtained from weight loss measurement for MS in 1 M HCl containing different concentrations of inhibitors at 308 K

Inhibitors	Concentration (ppm)	Corrosion rate (mg cm ⁻² h ⁻¹)	Surface coverage (θ)	η (%)
Blank	0.0	7.60	--	--
INH-1	5	2.52	0.6339	63.39
	10	2.06	0.7304	73.04
	15	1.56	0.7956	79.56
	20	1.10	0.8556	85.56
	25	0.63	0.9173	91.73
INH-2	5	2.23	0.7086	70.86
	10	1.93	0.7478	74.78
	15	1.43	0.8130	81.30
	20	0.93	0.8782	87.82
	25	0.56	0.9260	92.60
INH-3	5	1.90	0.7521	75.21
	10	1.36	0.8217	82.17
	15	0.86	0.8869	88.69
	20	0.63	0.9173	91.73
	25	0.30	0.9608	96.08
INH-4	5	1.20	0.8381	83.81
	10	0.83	0.8913	89.13
	15	0.53	0.9304	93.04
	20	0.30	0.9608	96.08
	25	0.13	0.9826	98.26

3.1.2. Effect of Inhibitor Concentration

In order to show the effect of temperature on inhibition efficiency of MS in 1M HCl, weight loss experiments were performed in temperature range of 308-338K in absence and presence of optimum concentration of inhibitors. Variation of inhibition efficiency with temperature is shown in Fig. 2(b). The corrosion rate, inhibition efficiency and surface coverage were calculated at each temperature and given in Table 3. Inspection of result showed that corrosion rate (C_R) increases with increasing the temperature. The inhibition efficiencies are found to decrease with increasing the solution temperature from 308 to 338

K. The decrease in inhibition efficiencies might be due desorption of adsorbed inhibitor film on the MS surface.

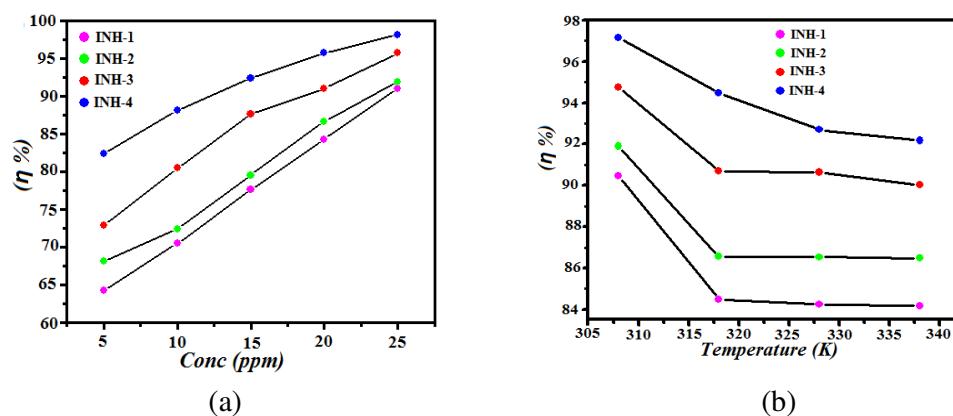


Fig. 2. (a) Inhibition efficiency of inhibitors at different concentration, (b) Inhibition efficiency of inhibitors at different temperature

Table 3. Inhibition parameters obtained from weight loss test for MS in 1 M HCl containing 25 ppm concentration of inhibitors at different temperatures

Inhibitors	Temperature (K)	Corrosion rate ($\text{mg cm}^{-2} \text{h}^{-1}$)	Surface coverage (η %)	(θ)
Blank	308	7.60	-	
	318	9.60	-	
	328	14.60	-	
	338	18.73	-	
INH-1	308	0.66	91.73	0.9173
	318	1.50	84.48	0.8448
	328	2.30	84.24	0.8424
	338	2.96	84.16	0.8416
INH-2	308	0.56	92.60	0.9260
	318	1.30	86.55	0.8655
	328	1.96	86.52	0.8652
	338	2.53	86.47	0.8647
INH-3	308	0.36	96.08	0.9608
	318	0.90	90.68	0.9068
	328	1.36	90.63	0.9063
	338	1.86	90.03	0.9003
INH-4	308	0.20	98.26	0.9826
	318	0.33	96.55	0.9655
	328	0.50	96.37	0.9637
	338	0.63	96.16	0.9616

3.1.3. Effect of Inhibitor Concentration

Basic information regarding interaction between inhibitors and MS can be derived with the help of various commonly used adsorption isotherms such as Langmuir, Temkin, Frumkin and Freundlich. In our present case several isotherms were tested but Langmuir isotherm

gives the best fit which gives a straight line between $\log(\theta/1-\theta)$ and $\log C$ (Fig. 3.a) with a regression coefficient nearly one.

Table 4. The values of K_{ads} and ΔG_{ads}° of optimum concentration of inhibitors for MS in 1M HCl at different temperature

Inhibitor	Temperature (K)	K_{ads} ($10^3 M^{-1}$)	$-\Delta G_{ads}^{\circ}$ (kJ mol ⁻¹)
INH-1	308	11.30	34.19
	318	6.49	33.03
	328	6.41	34.87
	338	6.11	35.79
INH-2	308	13.62	34.67
	318	7.72	34.29
	328	7.70	35.36
	338	7.67	36.43
INH-3	308	21.70	35.86
	318	11.68	35.39
	328	11.61	36.48
	338	10.48	37.40
INH-4	308	40.77	37.48
	318	33.59	38.18
	328	37.79	39.40
	338	34.21	40.63

The Langmuir isotherm is given by following relationship:

$$\frac{C_{(inh)}}{\theta} = \frac{1}{K_{(ads)}} + C_{(inh)} \quad (6)$$

where $C_{(inh)}$ is the inhibitor concentration and K_{ads} is the equilibrium constant for the adsorption–desorption process. The slopes for all four inhibitors were also found to be close to unity which confirmed the validity of the Langmuir adsorption isotherm. From the intercept of values the values of K_{ads} were calculated and given in Table 4.

It is apparent from the Table; the values of K_{ads} in presence of inhibitors are larger than in absence of inhibitors which suggests the strong adsorption of inhibitors on MS surface [17]. The Gibbs free energy of adsorption depends upon value K_{ads} and this dependency can be explained by following equation:

$$\Delta G_{ads}^{\circ} = -RT \ln(55.5K_{ads}) \quad (7)$$

where R is the gas constant and T is the absolute temperature (K). The value 55.5 represents the concentration of water in solution (mol L^{-1}) [18]. It is generally accepted that if values of ΔG_{ads}° are up to -20 kJ/mol then this type of adsorption can be regarded as physisorption, in which case adsorption results through the electrostatic interactions between the positively charged inhibitors molecules and the negatively charged MS surface. However, if values of ΔG_{ads}° are above -40 kJ/mol, then this type of adsorption are regarded as chemisorption, which is due to charge sharing or transfer from the inhibitor molecules to the metal surface to form a covalent bond [19-21]. In our present study the value of ΔG_{ads}° ranges in between 33.03–40.63 kJ/mol this result indicates that the adsorption of the inhibitor on MS surface involves both physical as well as chemical adsorption [22-23].

3.1.4. Thermodynamic and Activation Parameters

The thermodynamic and activation parameters were derived by performing the weight loss experiments at different temperature (308 -338K) in order to explain the mechanism of adsorption. The apparent activation energy (E_a) for dissolution of MS in 1M HCl can be expressed using the Arrhenius equation:

$$\log(C_R) = \frac{-E_a}{2.303RT} + \log \lambda \quad (8)$$

where E_a is the apparent activation energy (J mol^{-1}), R is the molar gas constant ($8.314 \text{ J K}^{-1} \text{ mol}^{-1}$), T is the absolute temperature (K), and λ is the Arrhenius pre-exponential factor. Fig. 3(b) gives a straight line between $\log C_R$ and $1/T$ (Arrhenius plot) in absence and presence of optimum concentration of inhibitors. From the slope of each line in Fig. 3(b), the apparent activation energies were calculated using equation, $E_a = (\text{slope}) \times 2.303R$ and given in Table 5. It is clear from the Table, that E_a in the presence of inhibitor are higher than those in the free acid solution indicating that investigated inhibitors exhibit low inhibition efficiencies at elevated temperatures [24]. The temperature dependency of corrosion rate can also be represented by another form of Arrhenius equation which is called as transition state equation:

$$C_R = \frac{RT}{Nh} \exp\left(\frac{\Delta S^*}{R}\right) \exp\left(-\frac{\Delta H^*}{RT}\right) \quad (9)$$

where ΔH^* the apparent enthalpy of activation, ΔS^* the apparent entropy of activation, h Planck's constant, and N the Avogadro number, respectively. Fig. 3(c) give a straight line between $\log C_R/T$ vs $1/T$ (Transition state plot) with a slope value of $-\Delta H^*/2.303R$ and intercept value of $[\log(R/Nh) + (\Delta S^*/2.303R)]$ from which the values of ΔH^* and ΔS^* have been calculated and given in Table 5. The inspection of the thermodynamic data reveals that ΔH^* values in presence of inhibitors are higher (29.22- 35.21 kJ mol⁻¹) than in absence (26.04 kJ mol⁻¹) of inhibitors which suggest the slow dissolution rate of MS in presence of inhibitors. It is also clear from Table 5, that ΔS^* value are higher (-111.1 to -142.87 J K⁻¹ mol⁻¹) than in blank acid solution (-148.9 J K⁻¹ mol⁻¹) suggesting that disorderness is increased on going from reactant to activated complex on metal/solution interface [25-27].

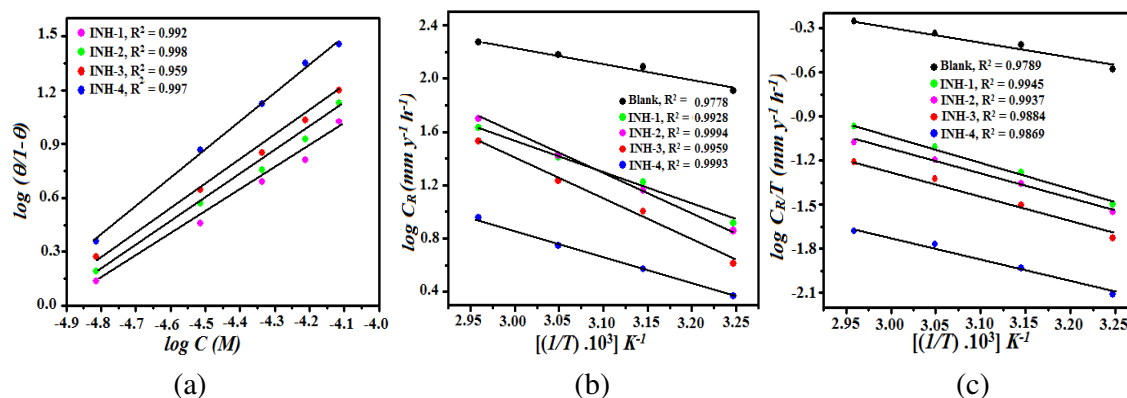


Fig. 3. (a) Langmuir adsorption isotherm, (b) Arrhenius plot ($\log C_R$ vs $1/T$), (c) Transition state plot ($\log C_R/T$ vs $1/T$)

Table 5. Values of E_a , ΔH , and ΔS of inhibitors for MS in 1 M HCl

Inhibitor	E_a (kJ mol ⁻¹)	ΔH (kJ mol ⁻¹)	ΔS (J K ⁻¹ mol ⁻¹)
Blank	28.48	26.04	-148.9
INH-1	46.83	35.21	-111.56
INH-2	55.56	31.36	-125.06
INH-3	38.83	29.22	-142.87
INH-4	59.85	34.53	-118.16

3.2. Electrochemical Measurements

3.2.1. Potentiodynamic Polarization Measurement

The anodic and cathodic Tafel polarization curves for MS corrosion in 1M HCl in absence and presence of optimum concentration of inhibitors is given in Fig. 4. The corrosion current densities were calculated by extrapolation of linear part of Tafel polarization curves. The potentiodynamic polarization parameters, namely, corrosion potential (E_{corr}), corrosion current density (I_{corr}), anodic Tafel slope (β_a), cathodic Tafel slope (β_c), and percentage inhibition efficiency (η %), calculated from the polarization curves are depicted in Table 6.

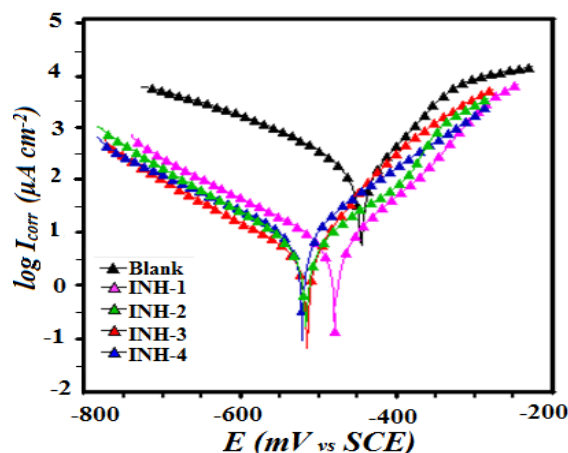


Fig. 4. Tafel polarization curves for corrosion of MS in 1 M HCl in the absence and presence of different concentration of inhibitors

It is apparent from the Table that the values of corrosion current density (I_{corr}) decreased in presence of inhibitors suggesting that the rate of electrochemical reaction was reduced due to the formation of protective layer of inhibitors molecules on MS surface. It is also clear that presence of inhibitors did not cause any significant change in E_{corr} values. It is described into literature [28] that if displacement in E_{corr} is > 85 mV in inhibited solution than that of uninhibited solution, the inhibitor can be classified as cathodic or anodic type. However, if the displacement in E_{corr} value is < 85 mV in presence of inhibitor than in absence of inhibitor, the inhibitor can be classified as mixed type. In present case maximum shift in E_{corr} value is 77 mV suggesting that investigated compounds are mixed type inhibitors [29]. From Table 6 it is observed that both cathodic and anodic reactions were affected in presence of inhibitors. However, the small shift in E_{corr} values in the positive direction with increasing concentration of inhibitor suggested that investigated inhibitors are mixed type predominantly anodic type.

Table 6. Potentiodynamic polarization parameters for MS in 1 M HCl solution containing optimum concentrations of inhibitors at 308

Tafel data							
<i>Inhibitor</i>	<i>conc</i>	<i>I_{corr}</i>	<i>E_{corr}</i>	<i>β_a</i>	<i>β_c</i>	<i>θ</i>	<i>η%</i>
	(ppm)	($\mu\text{A}/\text{cm}^2$)	(mV/SCE)	(mV/dec)	(mV/dec)		
Blank	0.0	1150	-445	70.5	114.6	---	---
INH-1	25	115.0	-522	103.6	196.2	0.9000	92.38
INH-2	25	69.45	-516	112.4	146.2	0.9396	93.96
INH-3	25	62.70	-479	89.4	136.1	0.9454	94.54
INH-4	25	11.50	-515	40.40	73.3	0.9900	99.00

3.2.2. Electrochemical Impedance Spectroscopy

Electrochemical impedance behavior of MS corrosion in 1M HCl in absence and presence of optimum concentration of inhibitors is given by a typical Nyquist plot [Fig. 5 (a)]. From the Nyquist plot depressed semicircles can be observed in which diameters of semicircle increases with inhibitors concentration showing that corrosion is mainly a charge transfer process [30]. Nyquist plots show a single semicircle capacitive loop in the higher frequency (*HF*) region and a very small inductive loop in the lower frequency (*LF*) region. The generation of HF capacitive loop is may be due to electron transfer reaction and time constant of the electric double layer and to the surface non-homogeneity of structural or interfacial origin, such as those found in adsorption processes. The LF inductive loop may be attributed to the relaxation process obtained by adsorption species like Cl^-_{ads} and H^+_{ads} on the electrode surface [31-33]. The values of impedance parameters namely charge transfer resistance (R_{ct}), solution resistance (R_s), phase Shift (n) double-layer capacitance (C_{dl}) and surface coverage (θ) obtained from the Nyquist plots and the calculated inhibition efficiencies are reported in Table 7. The electrochemical impedance parameters were derived by using equivalent circuit model as given in Fig. 5 (b), which consist of two resistances namely R_s (the resistance of solution between working electrode and counter electrode) and R_{ct} (charge transfer resistance). The double layer usually behaves as a constant-phase element (*CPE*) rather than as a pure capacitor. The deviation from ideal pure capacitor behavior may be due to surface heterogeneity which is generated from surface roughness, presence of impurities, formation of grain boundaries, adsorption of inhibitors and formation of porous layers [34]. The impedance of the *CPE* is expressed by:

$$Z_{CPE} = Q^{-1}(j\omega)^{-n} \quad (10)$$

where Q is the CPE coefficient, n the CPE exponent (phase shift) and j is a imaginary unit. For a double layer capacitance to behave like an ideal capacitor the value of n should be one [35]. It is observed from this Table 7 that R_{ct} values are higher in presence of inhibitors which is attributed to the formation of protective film at the metal/solution interface [36-37]. The decrease in C_{dl} value in presence of inhibitors shows the decrease in the local dielectric constant and/or an increase in the thickness of the electrical double layer. This finding suggests that inhibitors retard the corrosion process by forming a protective film on MS surface [38].

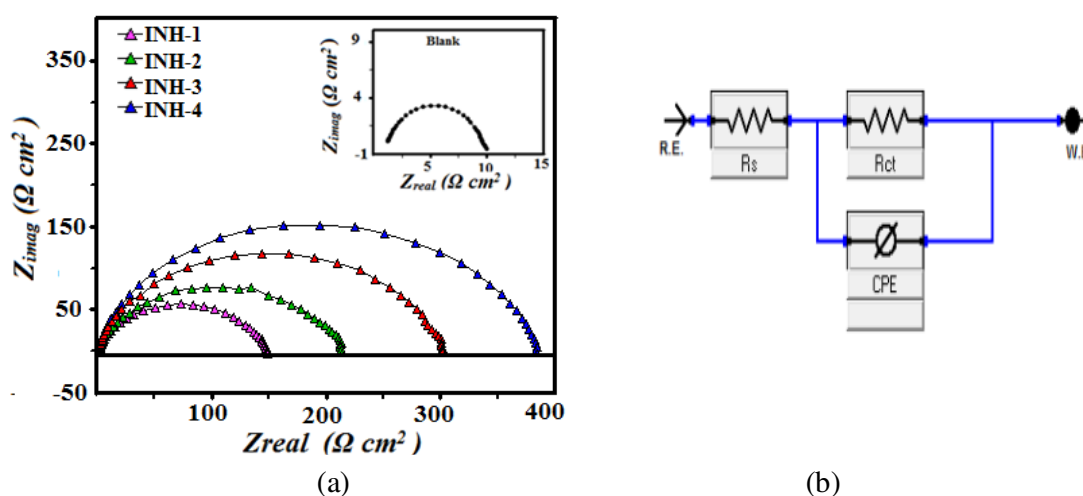


Fig. 5. (a) Nyquist plot in absence and presence of optimum concentration of inhibitors, (b) Equivalent circuit used to fit the electrochemical impedance data

In addition to Nyquist plot, Fig. 6 (a,b) shows the Bode impedance magnitude and phase angle plots recorded for the MS working electrode immersed in 1M HCl in the absence and presence of an optimum concentration of inhibitors at its OCP . In the Bode plot, a new phase angle shift in the higher-frequency range and a continuous increase in the phase angle shift with increasing concentration of inhibitors were observed. Shift in the phase angle provide solid information about corrosion inhibition performance. In general, the more negative value of phase angle associated with more inhibitive behavior of inhibitor [39]. It is seen from the Bode plots that in the intermediate frequency region, a linear relationship between $\log |Z|$ vs $\log f$ with a slope near -0.82 and the phase angle approaching -80° has been observed. The deviation from an ideal capacitive behavior (a slope value -1 and a phase angle value -90°) may be related to slowing of the rate of dissolution with time. The phase angle plot give a single maximum (one time constant) at around medium frequency zone and broadening of

this maximum in presence of inhibitors is due to formation of inhibitors film on MS surface [40].

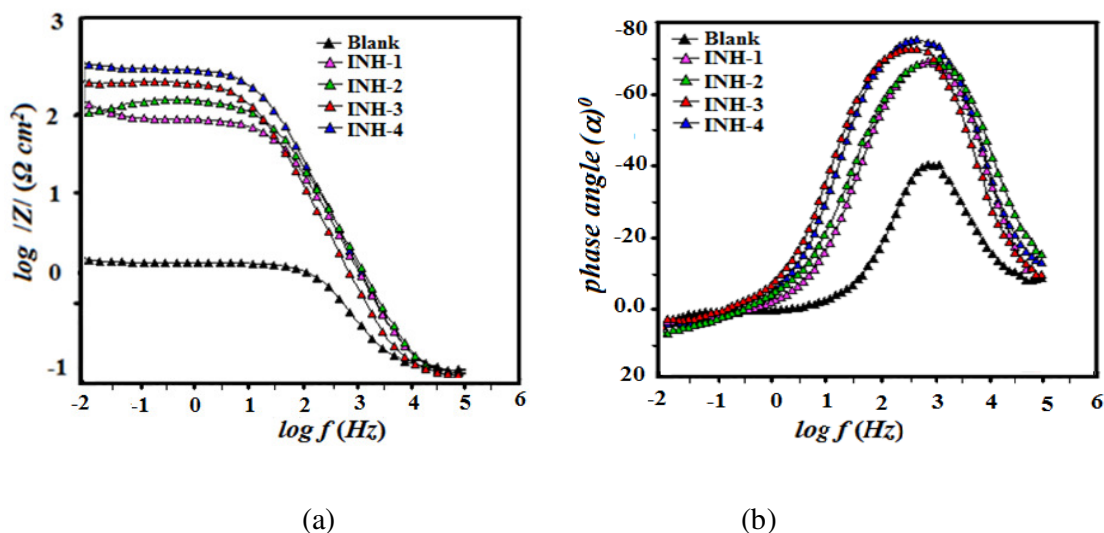


Fig. 6. (a) Between $\log |Z|$ and $\log f$, (b) Between phase angle and $\log f$

Table 7. Electrochemical impedance parameters obtained for MS in 1 M HCl in the absence and presence of optimum concentration of inhibitors at 308 K

<i>Inhibitor</i>	<i>conc</i> <i>ppm</i>	R_s ($\Omega\text{ cm}^2$)	R_{ct} ($\Omega\text{ cm}^2$)	n	Y_0 ($\mu\text{F cm}^{-2}$)	C_{dl} ($\mu\text{F cm}^{-2}$)	θ	$\eta\%$
Blank	0.0	1.12	9.58	0.827	249.8	106.21	---	---
INH-1	25	1.11	149.79	0.867	60.53	26.26	0.9360	93.60
INH-2	25	0.92	206.57	0.845	58.99	24.92	0.9536	95.36
INH-3	25	1.07	295.55	0.877	49.78	23.99	0.9675	96.75
INH-4	25	1.15	383.14	0.836	38.54	23.63	0.9749	97.49

3.3. Surface characterization

3.3.1. SEM Analysis

The SEM micrographs of the MS surfaces exposed to 1 M HCl without and with optimum concentration of inhibitors after 3h immersion time is shown in Fig. 7. Fig. 7 (a) represent the MS surface in absence of inhibitors in which the specimen surface was strongly damaged having a large number of cracks and pits due to strong corrosion of free mild. Fig. 7 (b-e) shows the SEM micrographs in presence of optimum concentration of different inhibitors. The inspection of the SEM micrographs reveals that the surface morphology is

remarkably improved in presence of inhibitors with little pits and cracks. This finding suggests that inhibitors retard the corrosion process by forming the protective film on metal surface.

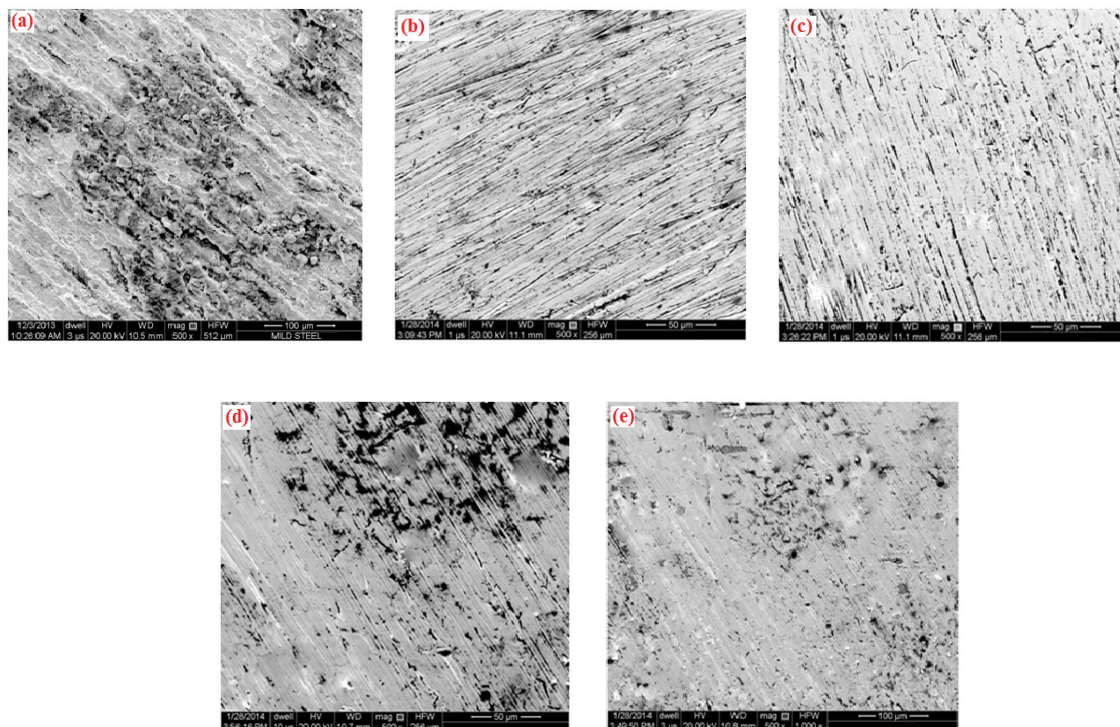


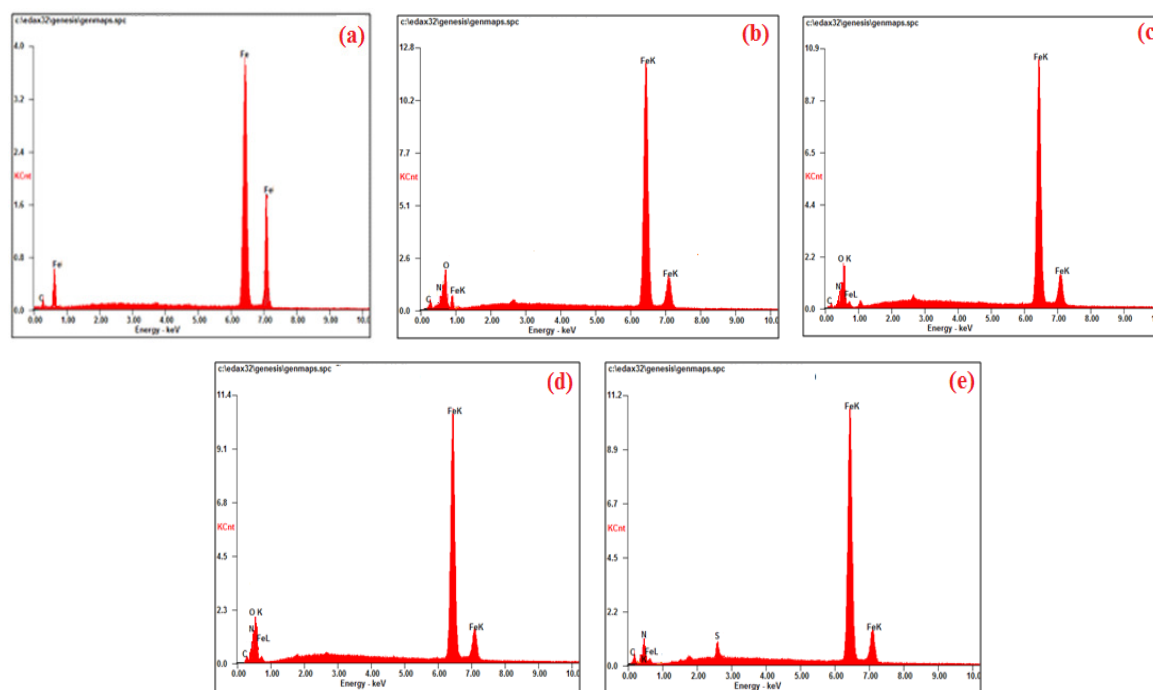
Fig. 7. SEM micrographs of MS surfaces (a) in 1M HCl without inhibitor, (b) in presence of INH-1, (c) in presence of INH-2, (d) in presence of INH-3, (e) in presence of INH-4

3.3.2. EDX Analysis

The formation of protective film of inhibitors on MS surface was also supported by EDX analysis. The EDX examination on MS surface was performed in absence and presence of optimum concentration of inhibitors. The percentage atomic content of MS samples obtained from EDX analysis is listed in Table 8. The results of EDX survey spectra are shown in Fig. 8. Fig. 8 (a) represents the EDX spectrum of MS specimens in absence of inhibitors. In EDX spectrum of uninhibited MS specimen, the peak of O is absent which confirms the dissolution of air-formed oxide film and free corrosion of bare metal. However, for inhibited solutions (Fig. 8.b–e), the EDX spectra showed an additional line characteristic for the existence of N, O and S (due to the N, O and S atoms of the inhibitors). The spectra of Fig. 8 (b–e) show that the Fe peaks are significantly suppressed relative to the abraded and uninhibited MS sample. The suppression of Fe lines occurs because of the overlying inhibitor film on MS surface

Table 8. Percentage atomic contents of elements obtained from EDX spectra for different inhibitors

Inhibitor	Fe	C	N	O	S
Blank	63.09	36.10	---	---	---
INH-1	68.62	27.24	1.35	2.63	---
INH-2	66.52	25.73	2.47	4.72	---
INH-3	64.22	24.13	3.75	7.65	---
INH-4	64.32	23.37	3.48	-----	7.95

**Fig. 8.** EDX spectra of MS surfaces, (a) in 1M HCl without inhibitor, (b) in presence of INH-1, (c) in presence of INH-2, (d) in presence of INH-3, (e) in presence of INH-4

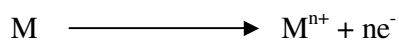
3.4. Mechanism of corrosion inhibition

Mechanism of corrosion inhibition in presence of chalcone and its heterocyclic derivatives can explain on the basis of molecular adsorption. The adsorption of inhibitors on metal surface depends upon various parameters mainly on the molecular structure. The inhibitor may adsorb on metal/electrolyte interface by: (1) electrostatic interaction between positively charged inhibitor and negatively charged chloride ions i.e. physisorption, (2) interaction between π - electrons of aromatic ring and functional groups with vacant d-orbital

of surface iron atoms i.e. chemisorption (3) interaction between unshared electron pair of heteroatoms and vacant d-orbital of surface iron atoms i.e. chemisorption and (4) interaction between d-electrons of iron atoms and vacant antibonding orbitals of heteroatoms i.e. retrodonation [41].

The process of corrosion inhibition take place in two steps:

(1) Anodic dissolution of MS in acid solution which can be represented as:



(2) Cathodic hydrogen evolution which can be represented as:



The potentiodynamic polarization studies reveals that investigated inhibitors are of mixed type i.e. they retard the anodic MS dissolution as well as cathodic hydrogen evolution [42]. It is well reported that in acidic media inhibitors containing heteroatoms exist as protonated form. The protonated form of inhibitors may adsorb directly on the cathodic site of MS and thus retard the hydrogen evolution, whereas the adsorption on the anodic site through p-electrons of aromatic ring as well as functional groups unshared heteroatoms takes place by which they retard the MS dissolution. Initially the protonated form of inhibitors start competing with the H^{+} ions for electrons on MS surface. After evolution of H_2 inhibitors molecules returns to their neutral form and chemical adsorption between nonbonding electrons of heteroatoms and d-orbitals of iron metal takes place. This type of interaction causes excessive accumulation of negative charge on MS surface and to relieve from extra negative charge the electrons are transferred from d-orbitals of surface iron atoms to anti bonding orbitals of the inhibitors (retro donation) [43]. Both weight loss and electrochemical measurements show that order of inhibition efficiencies four inhibitors are as follows: INH-4 > INH-3 > INH-2 > INH-1. This order of inhibition efficiency can be explain on the basis of molecular size and presence of electronegative atoms. It is well reported in literature that larger size and higher molecular weight favor the adsorption [44].

4. CONCLUSION

The results demonstrated that the investigated inhibitors behave as good inhibitors for mild steel in 1M HCl solution. Their efficiency increases with increase in concentration of inhibitors in 1M HCl. The adsorption of inhibitors on mild steel surface is found to obey the Langmuir adsorption. Negative values of free energies of adsorption suggest the spontaneous nature of adsorption of inhibitors on mild steel surface. The inhibiting efficiencies obtained by polarization, EIS, weight loss measurements and surface analyses are in good agreement.

REFERENCES

- [1] E. S. Ferreira, C. Giacomelli, F. C. Giacomelli, and A. Spinell, *Mater. Chem. Phys.* 83 (2004) 129.
- [2] M. Elachouri, M. S. Hajji, S. Kertit, E. M. Essassi, M. Salem, and R. Coudertll, *Corros. Sci.* 37 (1995) 381.
- [3] B. Mernari, H. Elattari, M. Traisnel, F. Bentiss, and M. Lagrenee, *Corros. Sci.* 40 (1998) 391.
- [4] E. M. Sherif, *Appl. Surf. Sci.* 252 (2006) 8615.
- [5] V. Lakshminarayanan, K. Kannan, and S. R. Rajagopalan, *J. Electroanal. Chem.* 364 (1994) 79.
- [6] S. Muralidharan, M. A. quraishi, and S. V. K Iyer, *Corros. Sci.* 37 (1995) 1739.
- [7] J. Cruz, R. Martinez, J. Genesca, and E. Garcia-Ochoa, *J. Electroanal. Chem.* 566 (2004) 111.
- [8] K. F. Khaled, K. Babic-Samardzija, and N. Hackerman, *Electrochim. Acta*, 50 (2005) 2515.
- [9] S. K. Shukla, and M. A. Quraishi, *Corros. Sci.* 51 (2009) 1007.
- [10] P. R. Roberge, *Corrosion inhibitors*, in: *Handbook of Corrosion Engineering*, McGraw-Hill, New York (1999) 833.
- [11] B. A. Bhat, K. L. Dhar, A. K. Saxena, and M. Shanmugavel, *Bioorg. Med. Chem.* 15 (2005) 177.
- [12] L. E. Michael, M. S. David, and S. S. Prasad, *J. Med. Chem.* 33 (1990) 1948.
- [13] S. Elayyoubi, B. Hammouti, H. Oudda, M. Zerfaoui, S. Kertit, and A. Bouyanzer, *Trans. Saes* 37 (2002) 29.
- [14] M. Bouklah, A. Bouyanzer, M. Benkaddour, B. Hammouti, A. Aouniti, and M. Oulmidi, *Bull. Electrochem* 19 (2003) 483.
- [15] M. J. Elarfi, and H. Al-Difar, *Sci. Revs. Chem. Commun.* 2 (2012) 103.
- [16] A. U. Ezeoke, O. G. Adeyemi, O. A. Akerele, and N. O. Obi-Egbedi, *Int. J. Electrochem. Sci.* 7 (2012) 533.
- [17] M. Lagrenee, B. Mernari, M. Bouanis, M. Traisnel, and F. Bentiss, *Corros. Sci.* 44 (2002) 573.
- [18] E. Khamis, F. Bellucci, R. M. Latanision, and E. S. H. El-Ashry, *Corrosion* 47 (1991) 677.
- [19] J. D. Talati, and D. K. Gandhi, *Corros. Sci.* 23 (1983) 1315.
- [20] Z. Szklarska-Smialowska, and J. Mankowski, *Corros. Sci.* 18 (1978) 953.
- [21] A. Yurt, S. Ulutas, and H. Dat, *Appl. Surf. Sci.* 253 (2006) 919.
- [22] A. Döner, R. Solmaz M. Özcan, and G. Kardas, *Corros. Sci.* 53 (2011) 2902.
- [23] P. R. Roberge, *Handbook of Corrosion Engineering*, McGraw-Hill, New York, 2000.
- [24] S. M. A. Hosseini, and A. Azimi, *Corros. Sci.* 51 (2009) 728.

- [25] N. Guan, M. L. Xueming, and L. Fei, *Mater. Chem. Phys.* 86 (2004) 59.
- [26] M. A. Quraishi, A. Singh, V. K. Singh, D. K. Yadav, and A. K. Singh, *Mater. Chem. Phys.* 122 (2010) 114.
- [27] B. G. Ateya, B. E. El-Anadauli, and F.M. El-Nizami, *Corros. Sci.* 24 (1984) 509.
- [28] W. H. Li, Q. He, C. L. Pei, B. R. Hou, *J. Appl. Electrochem.* 38 (2008) 289.
- [29] H. Ashassi-Sorkhabi, B. Shaabani, and D. Seifzadeh, *Appl. Surf. Sci.* 239 (2005) 154.
- [30] K. W. Tan, and M. J. A. Kassim, *Corros. Sci.* 53 (2011) 569.
- [31] R. S. Goncalves, D. S. Azambuja, and A. M. Serpa Lucho, *Corros. Sci.* 44 (2002) 467.
- [32] M. A. Amin, S. S. Abd El-Rehim, E. E. F. El-Sherbini, and R. S. Bayyomi, *Electrochim. Acta* 52 (2007) 3588.
- [33] M. A. Veloz, and I. Gonzalez, *Electrochim. Acta*, 48 (2002) 135.
- [34] A. Popova, E. Sokolova, S. Raicheva, and M. Christov, *Corros. Sci.* 45 (2003) 33.
- [35] H. Gohr, J. Schaller, and C. A. Schiller, *Electrochim. Acta* 38 (1993) 1961.
- [36] B. Mernari, H. Elattari, M. Traisnel, and F. Bentiss, *Corros. Sci.* 40 (1998) 391.
- [37] S. V. Ramesh, and A. V. Adhikari, *Mater. Chem. Phys.* 115 (2009) 618.
- [38] I. Ahamad, R. Prasad, and M. A. Quraishi, *Corros. Sci.* 52 (2010) 1472.
- [39] A. K. Singh, and M. A. Quraishi, *J. Appl. Chem.* 40 (2010) 1293.
- [40] H. H. Hassan, *Electrochim. Acta* 53 (2007) 1722.
- [41] M. E. Achouri, M. R. Infante, F. Izquierdo, and S. Kertit, *Corros. Sci.* 43 (2001) 19.
- [42] A. Yurt, A. Balaban, Ustun, S. Kandemir, G. Bereket, and B. Erk, *Mater. Chem. Phys.* 8 (2004) 420.
- [43] O. O. Xometl, N. V. Likhanova, M. A. D. Anguilar, E. Arce, H. Dorantes, and P. A. Lozada, *Mater. Chem. Phys.* 110 (2008) 344.
- [44] A. K. Singh, and M. A. Quraishi, *Corros. Sci.* 51 (2009) 2752.